Available online at www.sciencedirect.com

ScienceDirect

Ceramics International 34 (2008) 2143–2146

CERAMICS INTERNATIONAL

www.elsevier.com/locate/ceramint

Efficient upconversion luminescence of Er^{3+}:SrF_2–SiO_2–Al_2O_3 sol–gel glass ceramics

Yunlong Yu, Yuansheng Wang *, Daqin Chen, Feng Liu

State Key Laboratory of Structural Chemistry, Fujian Institute of Research on the Structure of Matter,
Chinese Academy of Sciences, Graduate School of Chinese Academy of Sciences, Fuzhou, Fujian 350002, China

Received 21 April 2007; received in revised form 25 July 2007; accepted 28 August 2007

Available online 25 September 2007

Abstract

Er^{3+}:SrF_2–SiO_2–Al_2O_3 transparent glass ceramic was prepared by a sol–gel method. The effect of Al^{3+} doping on the microstructures and luminescence properties of the materials was investigated by the X-ray diffraction (XRD), the transmission electron microscopy (TEM) and the absorption and luminescence spectra measurements. It was evident that Al^{3+} ions play an important role in improving the structure stability of the glass ceramic by suspending the crystallization of the oxide glassy matrix. The upconversion luminescence of the Al^{3+}-doped glass ceramic was greatly enhanced and visible by the naked eyes, which implies the potential application of this material in the field of solid-state displays.

© 2007 Elsevier Ltd and Techna Group S.r.l. All rights reserved.

Keywords: D. Glass ceramics; Luminescence; Microstructure; Sol–gel

1. Introduction

In recent decades, transparent oxyfluoride glass ceramics have been investigated widely because they not only have comparatively low phonon energies ascribed to fluorides, but also high chemical and mechanical stability related to oxides [1–3]. Sol–gel approach has been widely employed in preparing optical glasses and glass ceramics. The major advantages of the sol–gel process, compared to other techniques (such as melting quenching method) include the uniform phase distribution, the relatively low processing temperature and the low cost of fabrication [4,5]. In our previous studies, based on the sol–gel method, Er^{3+}-doped transparent glass ceramics containing MF_2 (M = Ba, Sr and Ca) nano-crystals were prepared [6–8]. Unfortunately, a mass of hydroxyl groups that is effective in quenching the luminescence [9] could not be completely eliminated for these samples. In order to enhance the rare earth ions luminescence in the sol–gel glass, several attempts have been performed [5,10,11]. A simple route is to heat the sample at a relative high temperature to reduce the hydroxyl groups, but it is usually limited by the partial crystallization of the oxide glassy matrix that may debase the transparency of the material. It was reported that, in glass system, Al^{3+} as the network intermediate ion may improve the structure stability of the glass by decreasing the non-bridging ions and building a continue network [12]. Furthermore, Al^{3+} co-doping can alleviate the luminescence quenching of active ions by modifying the ions environment, and increase the solubility of active ions in the silica glass host, which can significantly improve the luminescence properties of the active ions [13,14]. In this work, Er^{3+}:SiO_2–SrF_2–Al_2O_3 glass ceramics were prepared by the sol–gel method, and their structural characteristics and luminescence performances were investigated. Remarkably, benefited from Al^{3+} doping, an intense upconversion luminescence visible by the naked eyes was obtained.

2. Experimental

The process for preparing sol–gel samples are similar to that reported in our previous paper [7]. Tetraethylorthosilicate (TEOS) was dissolved in the ethyl alcohol (the resultant solution was denoted as TEOS solution). Strontium acetate and erbium acetate were dissolved in the trifluoroacetic acid (TFA)/ H_2O (the resultant solution was denoted as TFA solution). In order to introduce Al^{3+}, aluminum nitrate was added to TFA

---

* Corresponding author. Tel.: +86 591 8370 5402; fax: +86 591 8370 5402.
E-mail address: yswang@fjirsm.ac.cn (Y. Wang).

0272-8842/$34.00 © 2007 Elsevier Ltd and Techna Group S.r.l. All rights reserved.
doi:10.1016/j.ceramint.2007.08.001

solution. The TFA and TEOS solutions were then mixed up and added with the acetate acid as the catalysis with stirring for 4 h to form a homogeneous clear mixture. The resultant clear sol was then poured into vessels and allowed to form gels at room temperature. The gels were aged for 5 days at room temperature and finally dried in steps at different temperatures (30–155 °C) for 7 days. The samples used in this study have the compositions (in mol ratio) of $90SiO_2$–$10SrF_2$–$0.5ErF_3$ and $97.5(90SiO_2$–$10SrF_2)$–$2.5Al_2O_3$–$0.5ErF_3$, and were denoted as SS and SSA, respectively. To obtain the glass ceramics, the as-made xerogels were heat treated at 800 °C (denoted as SS800 and SSA800, respectively) and 1000 °C (denoted as SS1000 and SSA1000, respectively) for 1 h, respectively. The final samples are monolithic pieces of about 1 mm × 10 mm × 20 mm and transparent at sight.

The XRD analysis was performed on an X-ray powder diffractometer (DMAX2500) with Cu Kα1 radiation. The microstructure of the samples was studied by the transmission electron microscopy (JEM-2010) equipped with an energy dispersive X-ray spectroscope (EDS) and operated at 200 kV. The specific surface areas were measured using a micromeritics (ASAP 2020) instrument. The optical absorption spectra were recorded by an UV near-infrared spectrophotometer (Lambda900). The visible fluorescence emission was recorded on an Edinburgh Instruments FLS920 spectrofluorimeter excited by a 379 nm light from a 450 W stable xenon lamp. The upconversion luminescence was performed with a 976 nm laser diode, and detected by an Edinburgh Instrument FLS920 spectrofluorimeter. The fluorescence decay curve at 540 nm was recorded with an Edinburgh Instruments FLS920 spectrofluorimeter when excited at 379 nm by a microsecond pulsed flash lamp. All these experiments were carried out at room temperature.

3. Results and discussion

The as-made SS and SSA xerogels were all highly transparent. The SS sample became opaque when thermal treatment temperature exceeded 800 °C, while the SSA sample still kept its transparency after the thermal treatment temperature reached 1000 °C. Fig. 1 shows the XRD patterns of the SS and SSA samples heat treated at 800 and 1000 °C, respectively. It can be observed that the patterns for 800 °C heated SSA and SS and 1000 °C heated SSA are similar to each other, which present some cubic SrF_2 (JCPDS no. 86-2418) crystalline peaks among the amorphous hump, while the pattern for 1000 °C heated SS exhibits several additional hexagonal SiO_2 (JCPDS no. 82-0511) crystalline peaks. Based on the Scherrer formula, the sizes of the SrF_2 nano-crystals were estimated from the XRD peak widths and the results are listed in Table 1. It can be observed that the average sizes of the SrF_2 nano-crystal in these two samples heated at same temperature are close to each other. Therefore, we can conclude that the doping of Al^{3+} improves the structure stability of the SSA1000 by suspending the crystallization of the oxide glassy matrix, and the opaque of the SS1000 is possible due to the emergence of the large size hexagonal SiO_2 nano-crystals (about 45 nm).

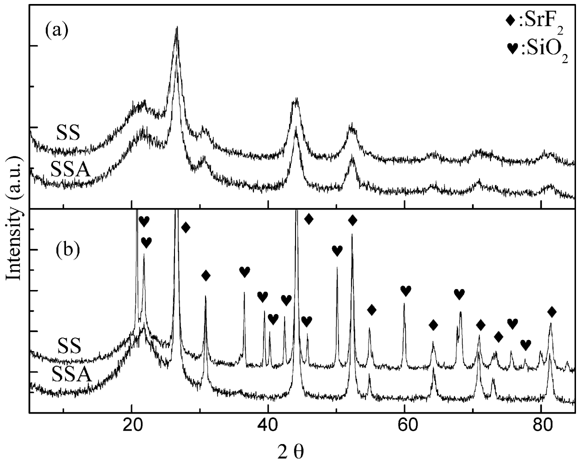

Fig. 1. XRD patterns of the SS and SSA samples heat treated at (a) 800 °C and (b) 1000 °C, respectively.

In SSA glass ceramic, Al^{3+} acts as a glass network former and replaces Si^{4+} to build up the continuous network. The presence of such network former results in the decrease of the non-bridging oxygen atoms, and thus raises the crystallization resistance of the oxide glassy matrix. Fig. 2 shows the TEM images and the corresponding selected area electron diffraction (SAED) pattern of the SSA samples heat treated at 800 and 1000 °C, respectively. It is found that for both samples homogeneously distributed SrF_2 spherical crystallites precipitated among the glass matrix and these nano-crystals grew with the increasing of the thermal treatment temperature.

The measured BET surface areas of as-made xerogels heated at 800 and 1000 °C are shown in Table 1. Noticeably, the BET surface area for SSA800 is less than a half of that for SS800, indicating that the doping of Al^{3+} enhances significantly the compactness of the material. With the heating temperature increases to 1000 °C, the BET surface area decreases dramatically, resulted from the elimination of the abundant micro-pores in the matrix.

The absorption spectra of three transparent glass ceramic samples SS800, SSA800 and SSA1000 are given in Fig. 3(a). The absorption peaks, corresponding to the transitions from the ground state $^4I_{15/2}$ to the specific excited states of Er^{3+}, are marked in the figure. For the samples of SS800 and SSA800, there is a remarkable absorption peak at about 1400 nm ascribing to the second Si–OH stretching vibration mode [7]. This peak disappears in SSA1000, implying the significant reducing of the OH^- content during the increasing of the temperature from 800 to 1000 °C. Compared with SSA800, SS800 presents a lower transparency window in the UV region owing to the existence of more residual pores in the glass matrix

Table 1
The average sizes of SrF_2 nano-crystals and the BET surface areas for the as-made xerogels SS and SSA heated at 800 and 1000 °C, respectively

	SS800	SSA800	SS1000	SSA1000
Crystallite size (nm)	11	13	23	20
BET surface areas (m^2)	100.4	41.9	14.2	3.8

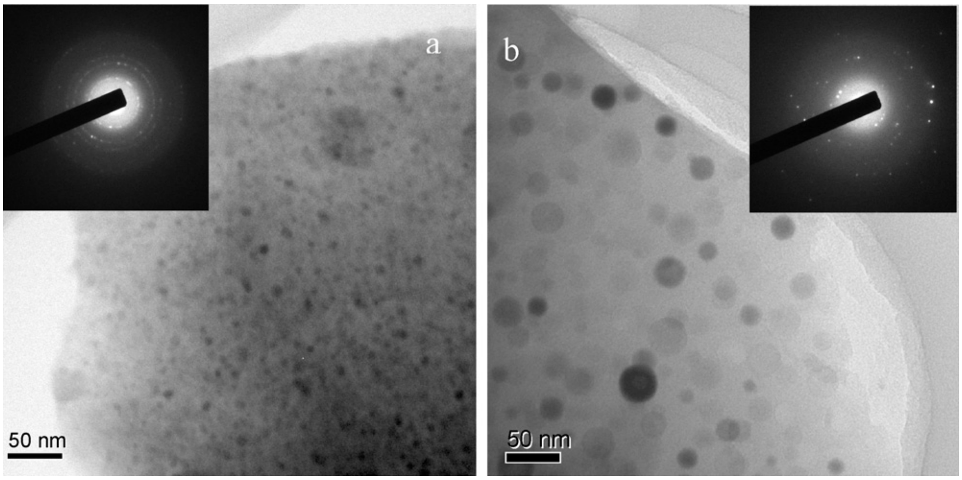

Fig. 2. TEM images of (a) SSA heated at 800 °C and (b) SSA heated at 1000 °C. The insets are the corresponding SAED pattern.

[4]. Further increasing thermal treatment temperature to 1000 °C, SSA1000 appears the highest transparence UV region due to little residual pores. In additional, according to the absorption spectra, the energy-level diagram of Er^{3+} ion was given in Fig. 3(b).

The downconversion and upconversion luminescence spectra of SSA1000 under 379 and 976 nm excitation, respectively are presented in Fig. 4. The emission bands can be assigned to $^2H_{11/2} \rightarrow {}^4I_{15/2}$ (522 nm), $^4S_{3/2} \rightarrow {}^4I_{15/2}$ (540 nm) and $^4F_{9/2} \rightarrow {}^4I_{15/2}$ (660 nm) transitions, respectively. The energy level diagram in Fig. 3(b) shows the possible transitions after Er^{3+} ions excited. By exciting at 379 nm, the Er^{3+} ions are directly excited to $^4G_{11/2}$. On the other hand, under 976 nm excitation, Er^{3+} ions are first excitation to the $^4I_{11/2}$ level by 976 nm photons, and then they can be excited to $^4F_{7/2}$ level by the ways of excited state absorption (ESA) and energy transfer (ET) [15]. After excitation to the $^4G_{11/2}$ or $^4F_{7/2}$ levels, the ions transferred rapidly and non-radiatively to the $^2H_{11/2}$ and $^4S_{3/2}$ levels. From these levels, most of the excited Er^{3+} ions decay radiatively to the ground state $^4I_{15/2}$ yielding the green emissions at 522 and 540 nm. In additional, some of them relax to the $^4F_{9/2}$ level by the multiphonon relaxation, and give rising to the red emission at 660 nm. In the inset of Fig. 4, fluorescence decay curve from the $^4S_{3/2}$ emitting level of Er^{3+} in SSA1000 is presented. The decay curve is well fitted to a single exponential function, giving $^4S_{3/2}$ lifetime of 32.8 μs.

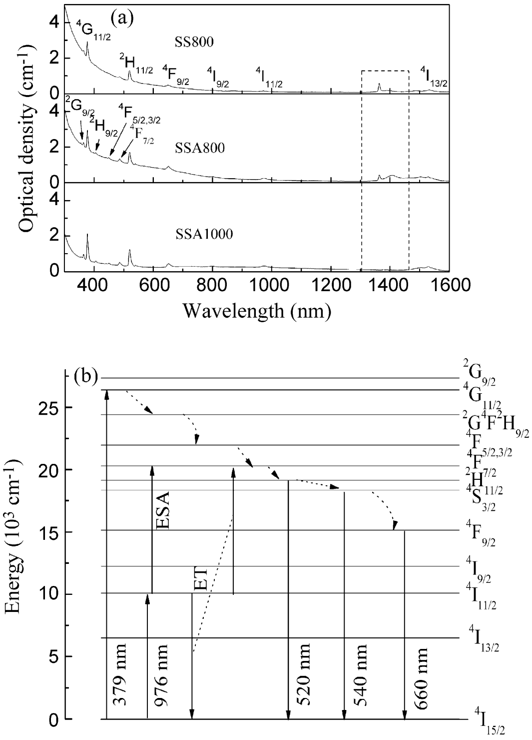

Fig. 3. (a) Room temperature absorption spectra of SS800, SSA800 and SSA1000, respectively. (b) Simplified energy-level diagram of Er^{3+} ions and the possible downconversion and upconversion mechanism.

It is well known that the luminescence for Er^{3+}-doped SiO_2 sol–gel glass usually shows a broadband emission at about 550 nm [15,16], however, in the present SSA1000 sample, obvious Stark splits are found for the green emission ($^4S_{3/2} \rightarrow {}^4I_{15/2}$), similar to those of Er^{3+}-doped glass ceramic

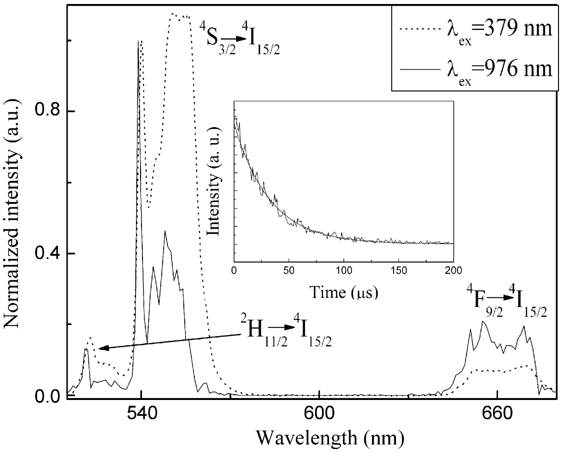

Fig. 4. The downconversion and upconversion luminescence spectra for SSA1000 under 379 and 976 nm excitation, respectively. The inset shows the fluorescence decay curve of $^4S_{3/2}$ level recorded at 540 nm (the fit curve is also included).

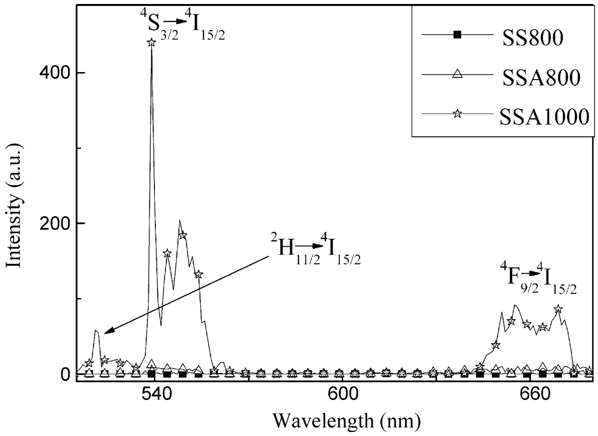

Fig. 5. The upconversion fluorescence spectra for SS800, SSA800 and SSA1000 under 976 nm excitation.

containing LaF_3 nano-crystals [17]. Therefore, it can be concluded that, at least, some Er^{3+} ions are partitioned into SrF_2 nano-crystals after crystallization. This is in accordance with the results of EDS analysis stated in Ref. [7], i.e. Er^{3+} ions tended to aggregate mainly inside or at the surface of the crystallites during crystallization. It is well known that the probability for non-radiative decay decreases exponentially with the number of required phonons [18]. The energy gap between $^4I_{11/2}$ and $^4I_{13/2}$ is about 3700 cm^{-1}, and approximate 10 phonons are required to produce non-radiative decay from $^4I_{11/2}$ to $^4I_{13/2}$ in fluoride nano-crystal with vibration energy about 300–400 cm^{-1} [19]. Since some Er^{3+} ions are located into SrF_2 nano-crystals (about 300 cm^{-1} [20]) for SSA1000 sample, the probability for non-radiative decay is thus very low, resulting in the efficient upconversion emissions. Compared to the upconversion emission excited by 976 nm, the relatively broad luminescence in the downconversion spectrum is due to the complementary emissions of Er^{3+} ions in the SrF_2 nano-crystals and the residual ones among the glass matrix under 379 nm excitation.

Fig. 5 shows the upconversion spectra of the transparent SS800, SSA800 and SSA1000 samples under 976 nm excitation. However, the upconversion fluorescence for SS800 is very weak and hardly detectable, while that for SSA800 is somewhat stronger. For the sample of SSA1000, it becomes very intense, and can be readily visible by the naked eyes Compared with SS800, the micro-pores in SSA800 are reduced due to the compaction of the matrix, which results in the weakening of the light scattering and consequently the enhancement of the upconversion luminescence. When further raising heat treatment temperature to 1000 °C, the drastic reducing of the micro-pores and the residual OH^- content certainly leads to much intense upconversion emissions.

4. Conclusion

In summary, Al^{3+} doping in the Er^{3+}:SrF_2–SiO_2 sol–gel transparent glass ceramic was found to improve the structure stability of the oxide glassy matrix, which makes the heat treatment of the glass ceramic at higher temperature to release the hydroxyl groups possible. Remarkably, very intense and visible upconversion luminescence was obtained in the glass ceramic heat treated at 1000 °C, which implies the possible application of this material in the field of solid-state displays.

Acknowledgements

This work was supported by the National Nature Science Foundation of China (no. 50672098) and the project of Nano-molecular Functional Materials of Fujian Province China (2005HZ01-1).

References

[1] M. Mortier, F. Auzel, J. Non-Cryst. Solids V 256–257 (1999) 361–365.
[2] V.K. Tikhomirov, J. Méndez-Ramos, V.D. Rodríguez, D. Furniss, A.B. Seddon, Opt. Mater. V 28 (2006) 1143–1146.
[3] A. Biswas, G.S. Maciel, R. Kapoor, C.S. Friend, P.N. Prasad, J. Non-Cryst. Solid 316 (2003) 393–397.
[4] A. Biswas, G.S. Maciel, R. Kapoor, C.S. Friend, P.N. Prasad, Appl. Phys. Lett. 82 (2003) 2389–2391.
[5] S.J.L. Ribeiro, C.C. Araújo, L.A. Burno, R.R. Goncalves, Y. Messaddeq, J. Non-Cryst. Solids 348 (2004) 180–184.
[6] D. Chen, Y. Wang, Y. Yu, E. Ma, L. Zhou, J. Solid State Chem. 179 (2006) 532–537.
[7] Y. Yu, D. Chen, Y. Wang, W. Luo, Y. Zheng, Y. Cheng, L. Zhou, Mater. Chem. Phys. 100 (2006) 241–245.
[8] L. Zhou, D. Chen, W. Luo, Y. Wang, Y. Yu, F. Liu, Mater. Lett. 61 (2007) 3988–3990.
[9] M. Fukushima, N. Managaki, M. Fuji, H. Yanagi, S. Hayashi, J. Appl. Phys. 98 (2005), 024316 (1–4).
[10] J.O. Kwon, S.I. Seok, D. Jung, J. Non-Cryst. Solids 352 (2006) 2841–2845.
[11] C. Strohhöfer, A. Polman, Appl. Phys. Lett. 81 (2002) 1414–1416.
[12] P.W. McMillan, Glass-Ceramics, 2nd ed., Academic press, New York, 1979, pp. 12–15.
[13] Y. Zhou, Y.L. Lam, S.S. Wang, H.L. Liu, C.H. Kam, Y.C. Chan, Appl. Phys. Lett. 71 (1997) 587–589.
[14] A. Monteil, S. Chaussedent, G. Alombert-Goget, N. Gaumer, J. Obriot, S.J.L. Ribeiro, Y. Messaddeq, A. Chiasera, M. Ferrari, J. Non-Cryst. Solids 348 (2004) 44–50.
[15] K. Tran Ngoc, H. Pham Thanh, C. Nguyen Duc, C. Armellini, A. Chiasera, M. Ferrari, Y. Jestin, M. Montagna, E. Moser, S. Pelli, G.C. Righini, Optoelectr. Lett. 2 (2006) 354–357.
[16] V.D. Rodríguez, J. Del Castillo, A.C. Yanes, J. Méndez-Ramos, M. Torres, J. Peraza, Opt. Mater. 29 (2007) 1557–1561.
[17] E. Ma, Z. Hu, Y. Wang, F. Bao, J. Lumin. 118 (2006) 131–138.
[18] T. Miyakawa, D.L. Dexter, Phys. Rev. B 1 (1970) 1961.
[19] S. Tanabe, H. Hayashi, T. Hanada, N. Onodera, Opt. Mater. 19 (2002) 343.
[20] R. Reisfeld, C.K. Jφrgensen, Laser and Excited States of Rare Earth, Springer-Verlag Press, New York, 1977, p. 99.